Kir4.1 K+ channels are regulated by external cations

Johan M. Edvinsson,[1,2] Anish J. Shah[2] and Lawrence G. Palmer[2,*]

[1]Graduate Program in Physiology, Biophysics and Systems Biology; [2]Department of Physiology and Biophysics; Weill Cornell Medical College; New York, NY USA

Key words: C-type inactivation, Cs block, NH_4 conductance, K-channel permeation, selectivity filter, K-buffering, K-channel gating

Abbreviations: Kir, inwardly rectifying potassium channel; NMDG, N-Methyl-D-Glucamine; K^+_o, extracellular K^+

The inwardly rectifying potassium channel (Kir), Kir4.1 mediates spatial K^+-buffering in the CNS. In this process the channel is potentially exposed to a large range of extracellular K^+ concentrations ($[K^+]_o$). We found that Kir4.1 is regulated by K^+_o. Increased $[K^+]_o$ leads to a slow (mins) increase in the whole-cell currents of Xenopus oocytes expressing Kir4.1. Conversely, removing K^+ from the bath solution results in a slow decrease of the currents. This regulation is not coupled to the pH_i-sensitive gate of the channel, nor does it require the presence of K67, a residue necessary for K^+_o-dependent regulation of Kir1.1. The voltage-dependent blockers Cs^+ and Ba^{2+} substitute for K^+ and prevent deactivation of the channel in the absence of K^+_o. Cs^+ blocks and regulates the channel with similar affinity, consistent with the regulatory sites being in the selectivity-filter of the channel. Although both Rb^+ and NH_4^+ permeate Kir4.1, only Rb^+ is able to regulate the channel. We conclude that Kir4.1 is regulated by ions interacting with specific sites in the selectivity filter. Using a kinetic model of the permeation process we show the plausibility of the channel's sensing the extracellular ionic environment through changes in the selectivity occupancy pattern, and that it is feasible for an ion with the selectivity properties of NH_4^+ to permeate the channel without inducing these changes.

Introduction

The inwardly rectifying potassium channels (Kir) are a family of channels mainly involved in K^+-vectoral transport and control of cell excitability. These channels are controlled by several factors, some that are general for the family (pH_i, lipids), and some that are specific for submembers (nucleotides, G-protein, intracellular Na^+ and extracellular K^+).[1]

Although all Kir-channels close in response to a decrease in intracellular pH, only a few do so in a physiologically relevant pH range (Kir1.1, Kir4.1, Kir4.2 and Kir4.x/5.1). Although the mechanism of pH-gating is not fully understood, it is known to involve closure of a region of the protein known as the bundle-crossing through large conformational changes in the channel protein.[2-5]

In addition to being gated by pH_i, Kir1.1 is regulated by K^+_o. This regulation, which has also been shown to occur in Kir4.2,[6] is manifested by a slow increase in whole-cell conductance when $[K^+]_o$ is elevated and conversely a slow decrease when $[K^+]_o$ is lowered. This phenomenon is different from the dependence of the open-channel conductance on the $[K^+]_o$ that is characteristic of Kir-channels and that happens immediately as the external solution is changed. Other ions that interact with the selectivity-filter of the channel, either blocking (Cs^+) or permeating (Rb^+) the

channel are able to mimic the effect of K^+.[7,8] This finding, in conjunction with mutational studies that have located residues in the selectivity-filter region necessary for this regulation to occur, have lead to the proposal that the selectivity filter acts as the sensor for the extracellular ionic milieu and possibly even as the gate.[8-10]

Structural and computational evidence has shown that the K^+-channel selectivity filter consists of five binding sites (S0–S4) with 2–3 sites occupied at any given time.[11-14] Under physiological conditions there is abundant K^+ available from the cytoplasm regardless of the $[K^+]_o$, hence if the selectivity filter senses changes in the ionic environment the mechanism must be more complex then a simple ligand binding reaction. In line with this it has been proposed that in similar K^+_o-dependent processes, such as C-type inactivation of Shaker channels and slow inactivation of KcsA channels, ions are sensed by the channel through changes in occupancy of a specific site or sites within the selectivity filter.[15,16] It is unclear if this hypothesis is consistent with the selectivity of the effect for different permeant and blocking ions.

Although pH_i and K^+_o may control different gates, there is a coupling between pH_i-gating and K^+_o-regulation of Kir1.1 that is apparent either as an increase of the pK_i when the $[K^+]_o$ is lowered or an inability to recover from a pH-closed state in the absence of K^+_o.[7,10,17,18] Although the mechanism of this interaction is not understood, a similar coupling exists between the state of

the bundle-crossing gate and the slow inactivation gate in KcsA and Shaker channels.[19-22] Furthermore, a lysine in the first transmembrane domain (K61 in Kir1.1b) is a main determinant of pH_i-sensitivity of Kir-channels[23-25] and is also involved in K^+_o-regulation of Kir1.1.[8,10] However, unlike in the case of pH_i-gating, where mutating this residue merely shifts the pK_i to lower values, K^+_o-dependent regulation is completely abolished if this residue is removed even if the pK_i is restored to normal values by introducing an additional mutation.[26]

In most physiological situations $[K^+]_o$ does not vary greatly. However, as the apical K-channel of principal cells in the cortical collecting duct of the nephron, Kir1.1 is exposed to large range of $[K^+]_o$. Thus this regulation may be physiologically relevant. Another case where sensitivity of a Kir-family member to changes in $[K]_o$ might be important involves K^+-spatial buffering in the CNS and Kir4.1.

In the CNS the K^+_o is controlled at around 3 mM.[27] However, during bursts of activity the extracellular K+-concentration can locally increase to about 10 mM[28] and under pathological conditions even higher.[27] One of the mechanisms to clear elevations of $[K^+]_o$ and prevent spontaneous neuronal firing or spreading depression is K+-spatial buffering.[29,30] This process takes advantage of the electrical coupling between glial cells to effectively transport K+ through the glial syncytium, from areas of high to low concentration. An increasing body of evidence suggests that the glial channel involved in this process is Kir4.1.[31-36] As this channel is closely related to Kir1.1 both by sequence homology and function, it is a likely candidate for K^+_o-regulation. In the present study we demonstrate and characterize K^+_o-dependent regulation of Kir4.1. Additionally, using a kinetic model of permeation we show that the changes in occupancy in the selectivity filter associated with changes in the ionic environment is consistent with the selectivity-filter's being the K+-sensor.

Results

Kir4.1 is regulated by K^+_o. To test if K^+_o-regulation occurs in Kir4.1 we incubated oocytes in solutions containing 1 mM K+ for 1 h prior to the start of the TEVC recording. After obtaining baseline whole-cell measurements in the 1 mM K+ solution, the bath solution was replaced with one containing 10 mM K+ and whole-cell currents were measured periodically. After 40 min, the bath solution was returned to 1 mM K+. To control for time-dependent effects not attributable to the solution changes during these long recordings some oocytes were kept in 1 mM K+ for the duration of the recording. As seen in **Figure 1C**, showing outward currents measured at 60 mV, there was a slow increase in the currents upon increasing $[K^+]_o$. The increase occurs uniformly throughout the voltage range tested (-150 mV to 100 mV) as seen in the representative IV curves in **Figure 1A**. We chose to plot outward currents as they have a smaller acute dependence on the extracellular ionic composition. This increase persists after the oocytes are returned to the 1 mM K+ solution. At this point (t = 50 min) the whole-cell currents, measured in the same solution, had increased 2.62 ± 0.33 (n = 6) fold compared to baseline (t = 5 min), whereas the time control did not change significantly;

0.86 ± 0.10 (n = 3). Executing the reverse protocol (**Fig. 1B and D**), i.e., incubating in 10 mM K+ and exposing the oocytes to 1 mM K+, resulted in a slow decrease (t = 50 min: 0.66 ± 0.06, n = 7) of the whole-cell currents, whereas the time control increased slightly (1.27 ± 0.10, n = 3).

Since we substituted the K+ in the bath solutions with Na+ it is possible that it was the increase in $[Na^+]_o$ rather than the decrease in $[K^+]_o$ that affected the whole-cell currents. To test this we compared the effects of the Na+-containing solution to that of one containing 109 mM N-Methyl-D-Glucamine (NMDG) (**Fig. 2**). NMDG is a large cation that is unlikely to affect the channel in a similar manner to the smaller Na+ or K+. We used 110 mM KCl as our baseline condition so that it would be identical for both groups. There is no significant difference in the fractional decrease in currents between the groups. Hence increased $[Na^+]_o$ is not downregulating the channel. Taken together these results demonstrate that Kir4.1 is regulated by K^+_o per se.

There is no coupling between Kir4.1 K^+_o-regulation and pH_i-sensitivity. The findings above indicate that Kir4.1 is regulated by external cations, similar to what has previously been found in Kir1.1. We next investigated if there exists a coupling between K^+_o-regulation and pH_i-sensitivity in Kir4.1 as has been found in Kir1.1.[7,10,17,18] A permeant acetate buffer was used to acidify the cytoplasm of intact oocytes expressing Kir4.1 [25] with either 10 mM or 110 mM K+ in the bath. In Kir1.1, decreasing $[K^+]_o$ causes an increase of the pK_i.[17] As evident in **Figure 3A**, this is not the case in Kir4.1 where we found a small but statistically significant increase in the pH_i-sensitivity in the 110 K+-solution.

To investigate this lack of coupling further, we introduced a mutation, K67M, into the N-terminal of Kir4.1. A homologous mutation in Kir1.1a, K80M, dramatically lowers the pK_i and completely abolishes the K^+_o-sensitivity of the channel.[37] As shown in **Figure 3A**, the K67M mutation had a similar effect on the pK_i of Kir4.1. It did not, however, decrease the K^+_o-sensitivity. The ratio of outward currents before and after exposure to 1 mM K+ for 45 min was 0.29 ± 0.08 for K67M (**Fig. 3B** and compared to 0.52 ± 0.09 for WT, **Fig. 2A**). Both these findings suggest that K^+_o-regulation in Kir4.1 does not depend on the state of the pH_i-sensitive gate.

Other pore-interacting ions can regulate Kir4.1. In the case of Kir1.1, other cations that interact with the channel pore, both permeable ions and voltage-dependent blockers, are able to mimic the effect on the whole-cell currents of K+. Before addressing the specificity of the effect of K+ on Kir4.1, we measured the selectivity of the channel to two ions that permeate most K+-channels, Rb+ and NH_4^+. The results from the ion substitution experiments are shown in **Figure 4**. Both ions had reduced conductance and permeability compared to K+. For Rb+, the conductance ratio was smaller than the permeability ratio, while the opposite was found for NH_4^+.

Next, we investigated the specificity of the effect of K^+_o on Kir4.1 using the protocol established above, but varying the cation in the low K+ bath solution. If the cation replacing K+ is able to mimic the effect of K^+_o, the decrease of currents will be less than that observed when the K^+_o is replaced with Na+ or NMDG+. **Figure 5** shows examples of this protocol using 110 Rb+ (A) and 110 NH_4^+ (B) in the bath. Rb+ was able to substitute for K+ and the
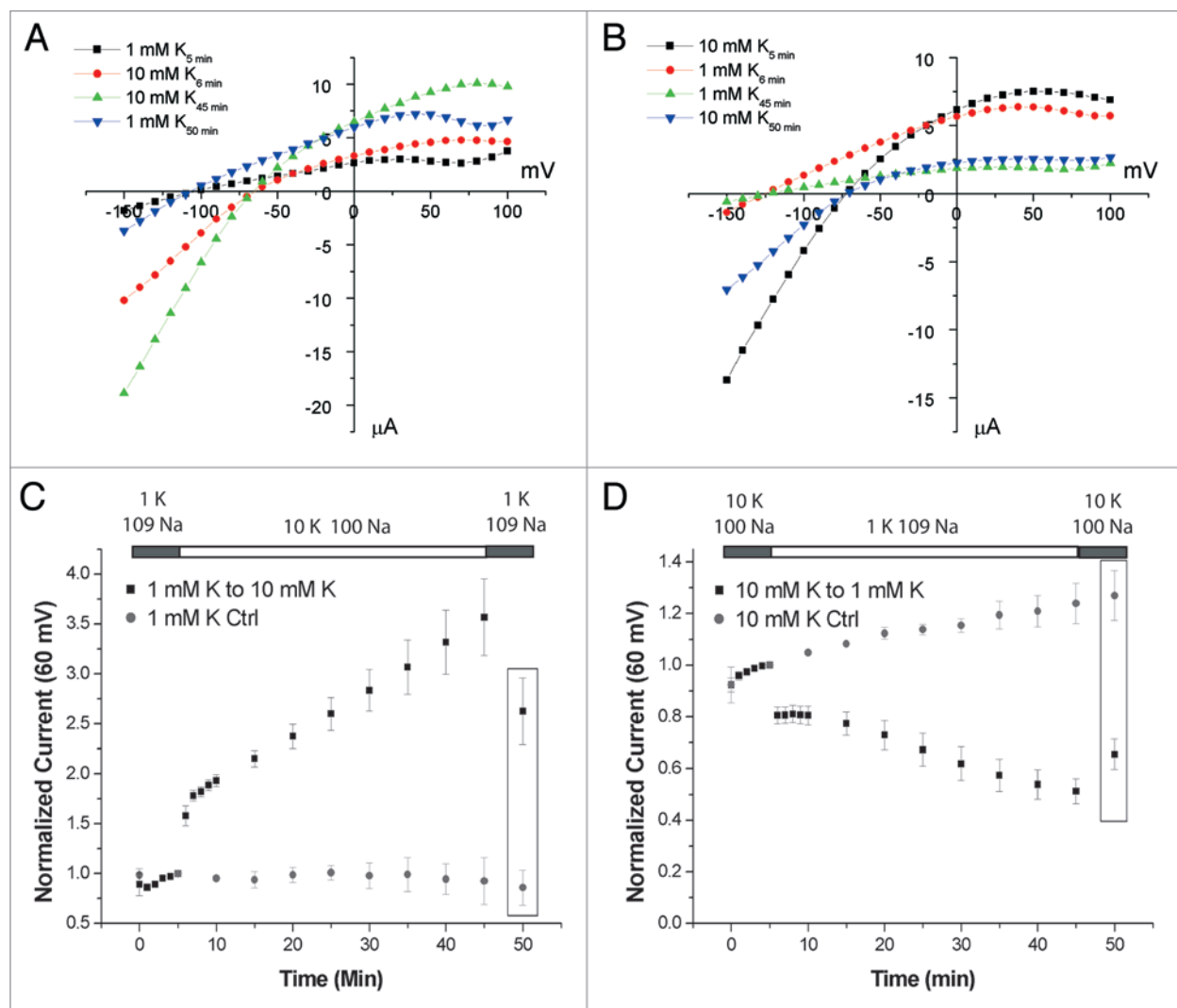
Figure 1. Kir4.1 is regulated by external K$^+$. Representative I-V relationships for switches from 1 K$^+$ to 10 K$^+$ (A) and 10 K$^+$ to 1 K$^+$ (B). Time points refer to (C and D) for (A and B) respectively. (C and D) Time course of measurements from oocytes preincubated in 1 mM (C) or 10 mM (D) K$^+$ for 1 h prior to the start of the experiment. The bath solution was switched to 10 mM (C) or 1 mM (D) K$^+$ after 5 min and then returned to the original solution after 45 min. The currents measured at 60 mV were normalized to the value at 5 min. Control oocytes were kept in the original solution for the duration of the recording period. Boxed in values are 2.62 ± 0.33 (n = 6) vs. 0.86 ± 0.10 (n = 3) for the control (p < 0.01) in (C) and 0.66 ± 0.06 (n = 7) vs. 1.27 ± 0.10 (n = 3) for the control (p < 0.001) in (D).

currents were stable or even increased slightly. NH$_4^+$, on the other hand, was not able to substitute for K$^+$ and the currents decreased. Since both these ions permeate the channel it follows that they must occupy the pore, but only Rb$^+$ is able to substitute for K$^+$ in keeping the channels in the open state. This suggests that the specific interaction between the sites in the selectivity filter and the given ions are important in order to maintain channel activity. We will discuss this issue further in the simulation section of the paper.

The solutions we tested in this manner are summarized in **Figure 5C** where we plot the currents after the bath solution was changed back to 110 mM K$^+$ (t = 50 min) relative to the baseline current (t = 5 min) under the same conditions. In this way we control for the acute effects that both blocking and permeant ions may have on the currents independent of the slow regulation studied in this paper.

Both the pore blocking ions, Cs$^+$ and Ba^{2+}, are able to substitute for the removed K$^+$ and prevent the decrease seen with 1 mM K$^+$ in the bath. In contrast to the permeant ions, the interaction between the channel and a blocking ion, in terms of pore occupancy, is more straightforward; when the channel is blocked, the blocking ion is occupying the pore. This allows us to correlate occupancy of the pore and regulation of the channel by Cs$^+$. First we measured Cs$^+$-block with 1 mM K$^+$ in the bath, a concentration that led to a decrease in the currents in the regulation experiments (**Fig. 6A and B**).

To measure regulation by Cs$^+$, we preincubated oocytes in 110 mM K$^+$ before adding 1 mM K$^+$ and varying Cs$^+$ concentrations to the bath. After 40 min the bath solution was returned to 110 mM K$^+$, whole-cell currents were measured and normalized to the initial currents in 110 mM K$^+$. Since occupancy of
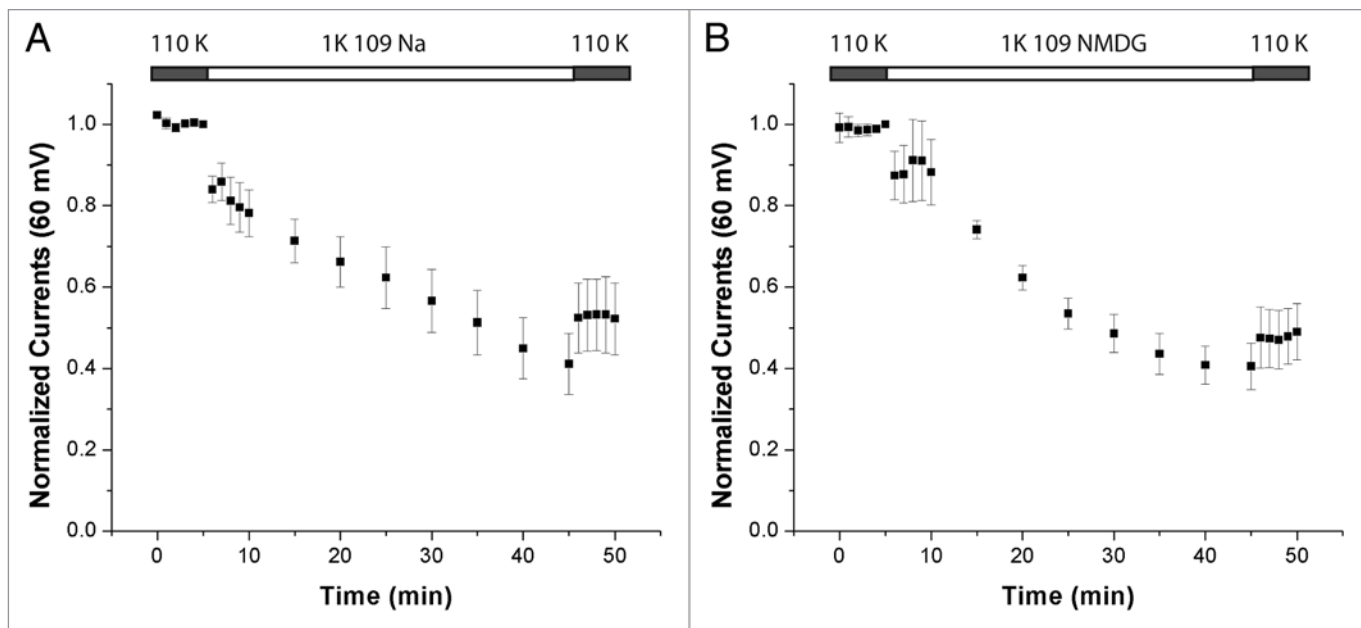
Figure 2. Kir4.1 is sensitive to the removal of K^+. Time courses of whole-cell currents were measured for oocytes preincubated in 110 mM K^+ for 1 hour prior to the start of the recording then switched to 1 K^+ and 109 Na^+ (A) or 1 K^+ and 109 $NMDG^+$ (B). The decreases in the current were 0.52 ± 0.09 for Na^+ (n = 5) and 0.47 ± 0.07 for $NMDG^+$ (n = 7). The difference between the two conditions is not significant (p > 0.6).
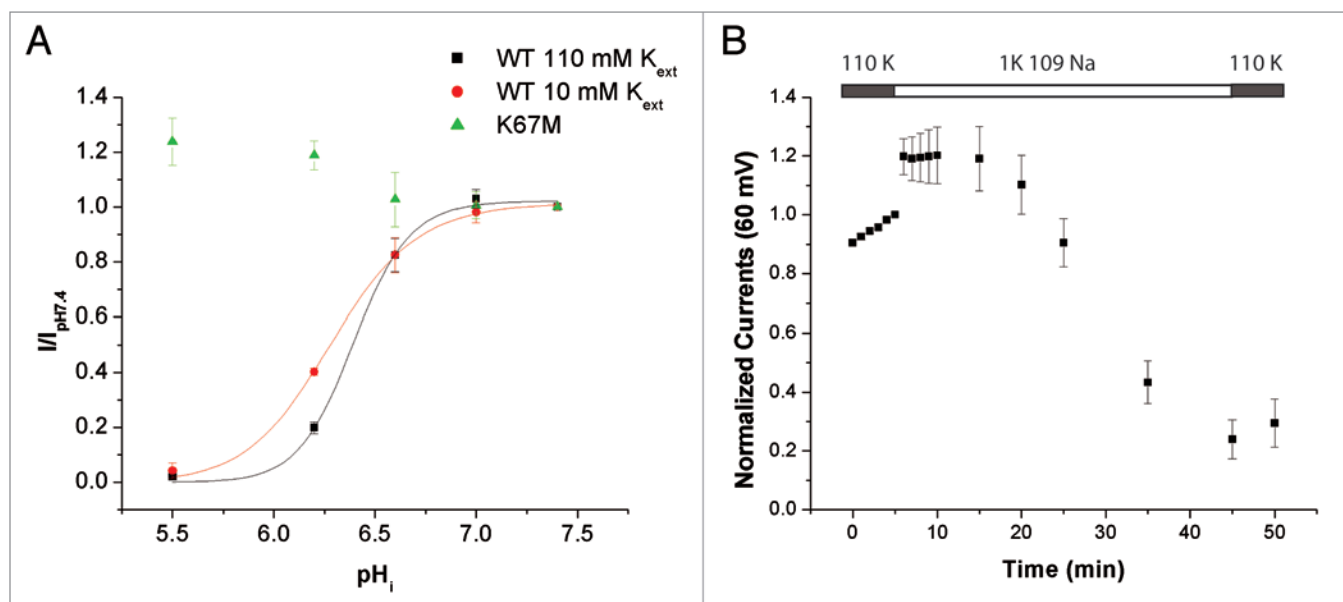

Figure 3. pH-sensitivity and K^+_o-regulation in Kir4.1. (A) pH_i-sensitivity at different $[K^+]_o$. The oocytes were acidified using permeable acetate buffer. pH_i was calculated from pH_o as described in the methods. The data were fitted with a Hill equation (110 K: pKa = 6.40 ± 0.01, n_h = 3.4 ± 0.5, n = 6; 10K: pKa = 6.28 ± 0.01, n_h = 2.3 ± 0.4, n = 4; pKa's are significantly different p < 0.0001). (B) Oocytes expressing Kir4.1 K67M were incubated in 110 mM K^+ for 1 h prior to start of the TEVC recording. The bath solution was switched to 1 mM K^+ at t = 6 min and returned to 110 mM K^+ at t = 46 min. Value at t = 50 min: 0.29 ± 0.08 n = 7.

the pore, like block, is a voltage dependent process the oocytes were clamped at -120 mV during the 40 min exposure period. The time course for the activation experiments are plotted in **Figure 6C**. The concentration dependencies of block and regulation by Cs^+ at -120 mV are plotted in **Figure 6D**. There is a reasonable agreement between the two measures, consistent with the idea that Cs^+ blocks and regulates the channel at the same site, presumably within the selectivity filter.

Single-channel currents. To better understand the process of K permeation through Kir4.1, we measured single-channel currents in cell-attached patches under conditions of low, intermediate and high K^+ concentrations in the patch-clamp pipette.
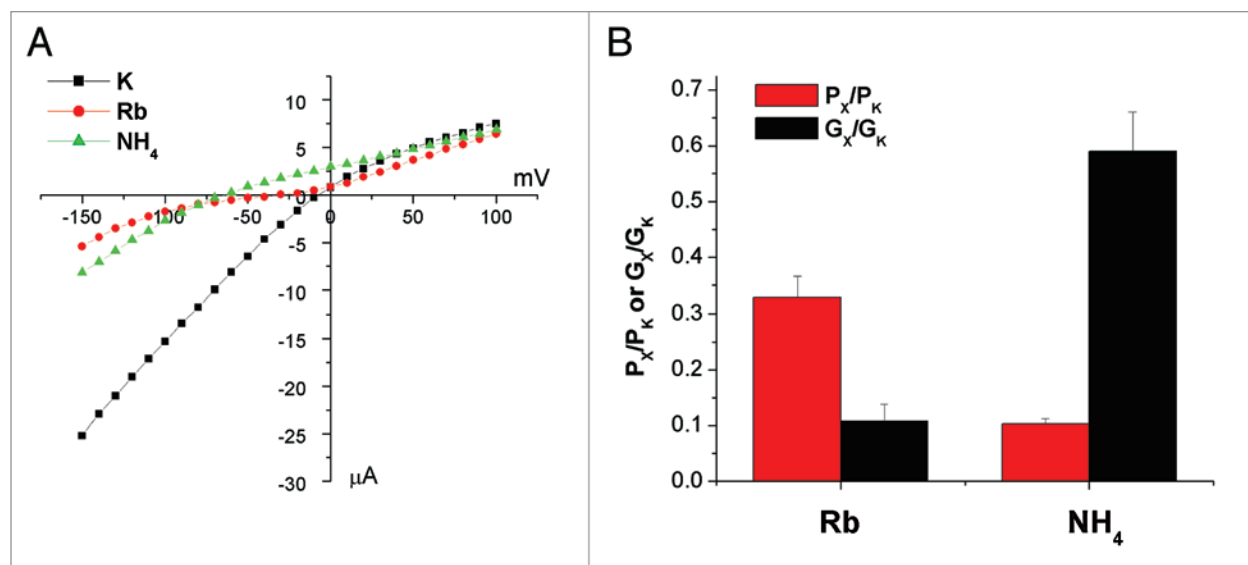
Figure 4. Kir 4.1 selectivity. Representative I-V plots with 110 mM K$^+$, Rb$^+$ or NH$_4^+$ in the bath. (B) Summary of the data from the ion-substitution experiments. G$_x$/G$_K$ was measured from the inward slope conductance 50 mV negative to the E$_{rev}$ for each condition. P$_x$/P$_K$ was calculated from the change in E$_{rev}$ when the test ion completely replaced K$^+$ in the bath using: P$_x$/P$_K$ = exp((ΔErev·F)/(R·T)). Data represent means ± SEM for seven experiments.

Results are shown in **Figure** 7. With high (110 mM) K$^+$, the inward conductance was 23 pS, similar to previous results.[38,39] We were unable to detect outward single-channel currents under these conditions. The inward conductance was a saturating function of K$^+$ with an estimated g$_{max}$ of 24.4 pS and an apparent K$_m$ of 16.7 mM.

Simulations. Our data suggest that the channel directly senses the extracellular ionic composition in the selectivity filter. As mentioned above this cannot simply be a matter of a general occupancy of ions in the selectivity filter, as even under low [K$^+$]$_o$ there are abundant K$^+$-ions available from the cytoplasm that has a constant high [K$^+$]. Current kinetic models of K$^+$-channel permeation, based on both structural[11,14] and computational[12,13] studies, are often represented with six binding sites (four in the selectivity filter of the channel (S1–S4) one in the extracellular vestibule (S0) and one in the central cavity of the channel (SC)) that are occupied by 2–3 ions at any given time. In a multisite pore such as this, we suggest that rather than the general presence of ions in the pore, a specific site or sites within the pore needs to be occupied to prevent deactivation of the channel.

To investigate if this is a plausible mechanism for K^+_o-dependent regulation in Kir4.1, we constructed a kinetic model using a 6-site model with five states (**Fig. 8A**) similar to that proposed previously in references 40 and 41. We fit the model to the data by altering the binding energies for the site and the energy barrier between them as this limited the amount parameters, particularly once the model was expanded to accommodate two ionic species. These parameters were then used to calculate rate constants.

We first investigated changes in occupancy induced by [K$^+$]$_o$ itself. Fitting the model to single-channel currents from cell-attached patches at three different [K$^+$]$_o$ (**Fig. 7**), we found a family of solutions that fit the data well and also predicted a relatively linear

i-V curve in symmetrical K$^+$ even outside the voltage region used for the fit. The parameters are listed in **Supplemental Table 1**. The i-V relationships for [K$^+$]$_o$ = 10, 40 and 110 mM at constant [K$^+$]$_{in}$ (110 mM), calculated using the mean parameter values, are shown in **Supplemental Figure 1A**, together with the measured values.

[K$^+$]$_o$ dependent changes in occupancy at the reversal potential are shown in **Supplemental Figure 1B** and summarized in **Figure 8B**. The reversal potential was the most relevant voltage domain since in our experiments the oocytes are unclamped and the high K$^+$ conductance keeps the voltage close to the equilibrium potential for K$^+$. Increasing [K$^+$]$_o$ leads to a decrease in occupancy of S2/S4 and an increase in the occupancy of S1/S3 and S0. This is a robust result that pertains generally to most solutions to the observed i-V relationships. The increase in occupancy of S0 directly reflects the equilibration of this site with external K$^+$. The increases in S1/S3 are largely due to changes in membrane potential that shift the ions from the S2/S4 position at less negative voltages.

Next we investigated the effects of Cs$^+$ by expanding the model to accommodate two ionic species. The resulting model has 32-states, since each ion in the pore as shown in **Figure 8A** can be either K$^+$ or Cs$^+$. We assumed that the number of Cs$^+$ binding sites and their placement in the electrical field are identical to those of K$^+$. We fit the model to the blocking data shown in **Figure 5B** over the voltage range -150 to 0 mV, using the parameters for K$^+$ from **Figure S1A** and altering the parameters for Cs$^+$. These data can be fitted in either of two general ways with average and variance for each shown in **Supplemental Table 1**. **Figure S1C** shows simulated voltage-dependent blocking curves at different [Cs$^+$]$_o$ for one of these cases. As was observed with K$^+$ there is an increase in S1/S3 occupancy with increasing [Cs$^+$]$_o$. Another set of parameters shown in **Supplemental Table 1** predicts increased
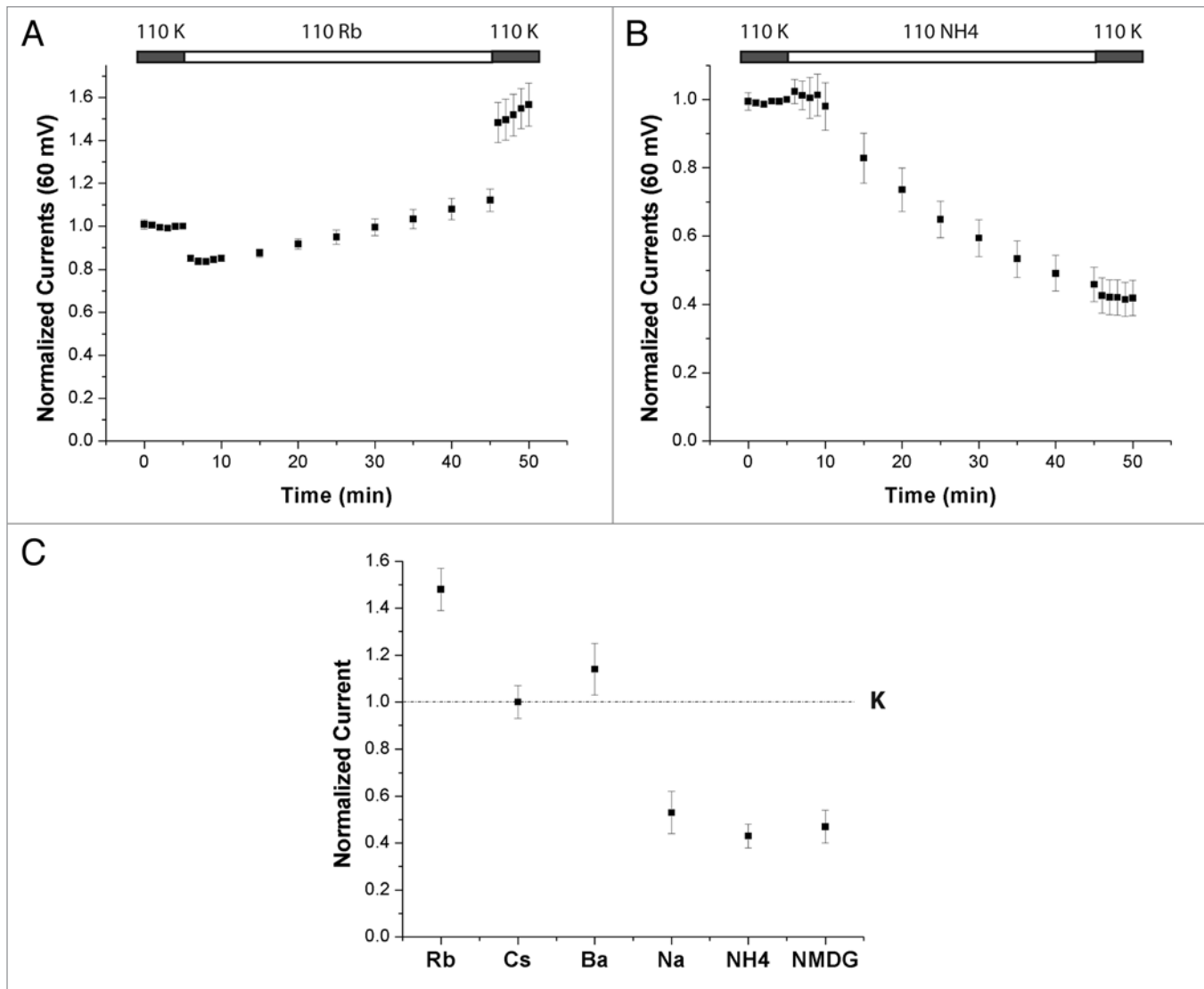
Figure 5. Other cations can mimic the effect of K^+_o. Oocytes were preincubated in 110 mM K^+ and the medium was switched to 110 mM Rb^+ (A) or 110 mM NH_4^+ (B) at t = 5 min. At t = 45 min the bath solutions were returned to 110 mM K^+. (C) Summary of responses to all ions tested as in (A and B). For details on the solution composition please refer to the method section. Currents measured when the bath solution was returned to 110 mM K^+ (t = 46 min) normalized to the 110 mM K^+ baseline (5 min). Data represent means ± SEM for 5–7 experiments.

binding in S2/S4. However, data from x-ray crystallography favor the increased S1/S3 scenario (see Discussion). The predicted changes in occupancies for addition of 10 mM Cs^+ in the presence of 1 mM K are summarized in **Figure 8B**.

Lastly, we examined NH_4^+, an ion that permeates the channel but is not able to prevent its inactivation. We again assume that the number of binding sites and their placement in the electrical field are identical to those of K^+, and that the macroscopic conductance ratio (**Fig. 5**) reflects changes in the single-channel conductance. The model was fit to the average NH_4^+ currents from the selectivity experiments scaled to the K^+ single-channel data. Parameter values are given in **Supplemental Table 1. Figure S1F** shows the i-V relationship for the 95 fits that converged to a solution. The change in the occupancies of the binding sites with addition of NH_4^+ to the extracellular side is shown in

Supplemental Figure 1F and summarized for the case of 110 mM NH_4^+ in **Figure 8B**. S0 occupancy increased similar to that calculated for K^+, but S1/S3 occupancy did not.

Discussion

We have demonstrated for the first time direct regulation of Kir4.1 by external cations. Although the physiological significance of this regulation is unknown, in the CNS, where Kir4.1 is expressed, areas of high neuronal activity can experience a local increase of $[K^+]_o$. During periods of high activity the $[K^+]_o$ can rise to around 12 mM[28] and during pathological conditions as high as 60 mM.[27] One of the proposed mechanisms to prevent this build up of $[K^+]_o$, and the potential for seizures and spreading depressions that follow is known as K^+ spatial buffering.[29,30]
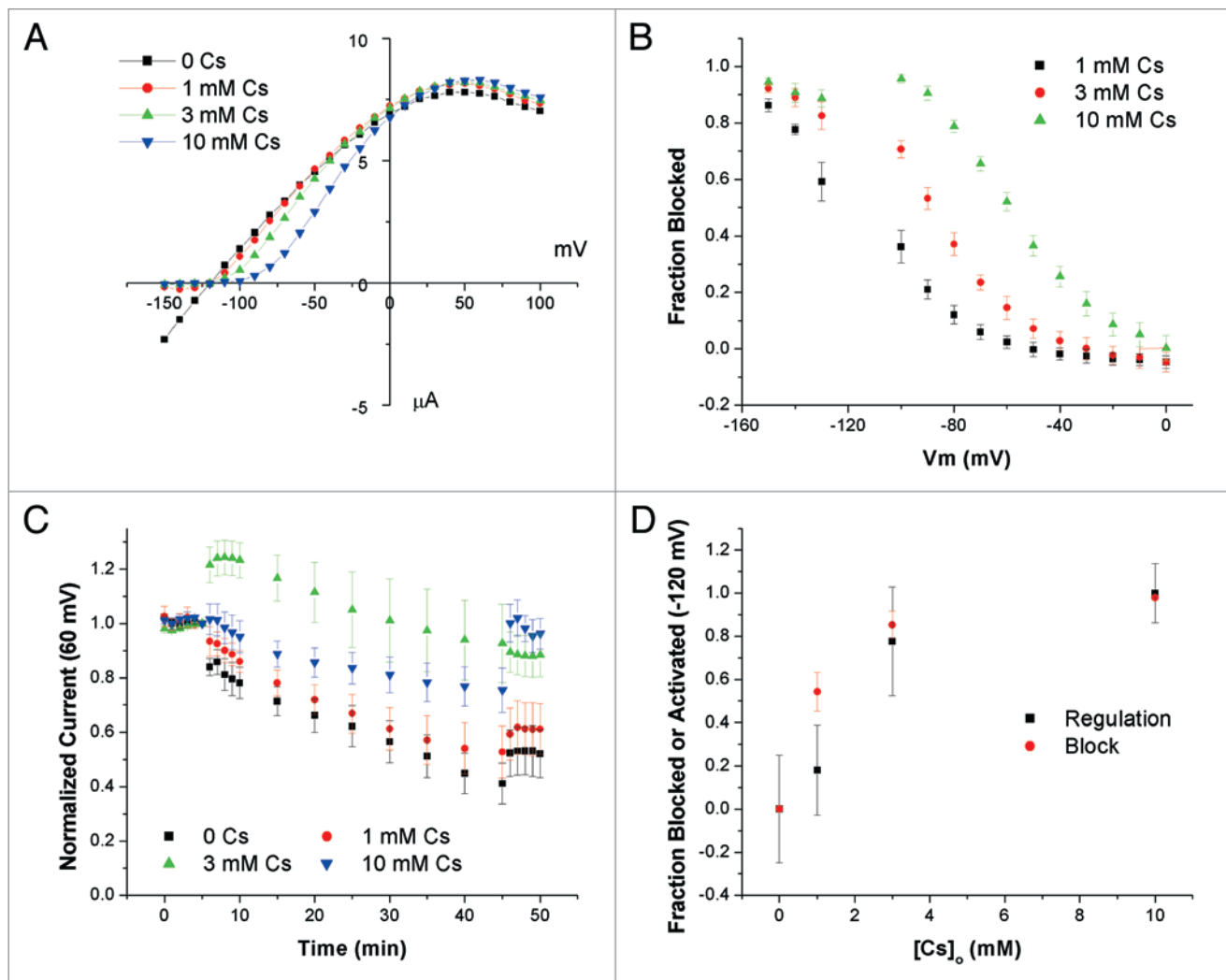
Figure 6. Comparing Cs+ block and regulation occur at similar concentrations. (A) Representative I-V relationships at different $[Cs^+]_o$. $[K^+]_o$ was constant at 1 mM K+. (B) Summary of Cs+ block experiments. Fractional block was computed as 1 - I(Cs)/I(0), where I(Cs) and I(0) are the currents in the presence and absence of Cs+, respectively. (C) Time course of whole-cell currents of oocytes preincubated in 110 mM K+ and switched to solutions containing 1 mM K+, 109 mM Na+ and indicated $[Cs^+]_o$ at t = 6 min. Currents are normalized to values at t = 5 min. The membrane voltage was clamped at -120 mV between t = 6 and t = 45 min (n = 4–6). (D) Summary plot Concentration dependence of regulation and block. Data for regulation are taken at t = 46 min and set to be 0 at 0 $[Cs^+]_o$ and 1 at 10 mM $[Cs^+]_o$. Data for block are interpolated values for -120 mV.

Influx of K+ into glial cells exposed to the elevated $[K^+]_o$ will depolarize both that cell and the entire electrically coupled syncytium. This will create a driving force for efflux of K+ in the areas not exposed to the elevated $[K^+]_o$, clearing K+ from the areas of K+ accumulation. Evidence points to Kir4.1 as the K+-channel involved in this clearance.[31-36] The K^+_o-dependent regulation that we have demonstrated offers a means to selectively upregulate the channels exposed to the elevated $[K^+]_o$.

Our data suggest that the selectivity filter of the channel directly senses the changes in the ionic composition of the extracellular solution. This is based on two observations: (i) only ions that interact with the selectivity-filter can substitute for K+; (ii) both permeant and voltage dependent blockers can substitute for K+. Since voltage-dependent blockers bind inside the electric field, i.e., the selectivity-filter,[42] and do not permeate the channel at a significant rate, it is unlikely that this process requires actual movement of ions across the membrane. Our data comparing Cs+-block and Cs+-regulation of Kir4.1 are consistent with the idea that these processes require occupancy of the same site or sites.

The idea that occupancy of a specific site within the selectivity filter controls the activity of the channel has been proposed for KcsA and Shaker channels.[16,19,43,44] We propose here that a similar mechanism occurs in Kir4.1. In our kinetic model, we found that increasing $[K^+]_o$ increases occupancy of the S0, and the S1/S3 sites. At a first glance this seems to contradict the results of MD-simulations of KcsA, where S2 occupancy appears to keep the selectivity filter in the conducting state.[16] However a recent computational study based on the KirBac1.1 structure suggests that even though S2 is the site where the closure of the filter occurs, this process is initiated from the S2–S4 configuration by flickering behavior from the ion in S2 into either S1 or S3.[15] S1/S3 occupancy could prevent this process, which could
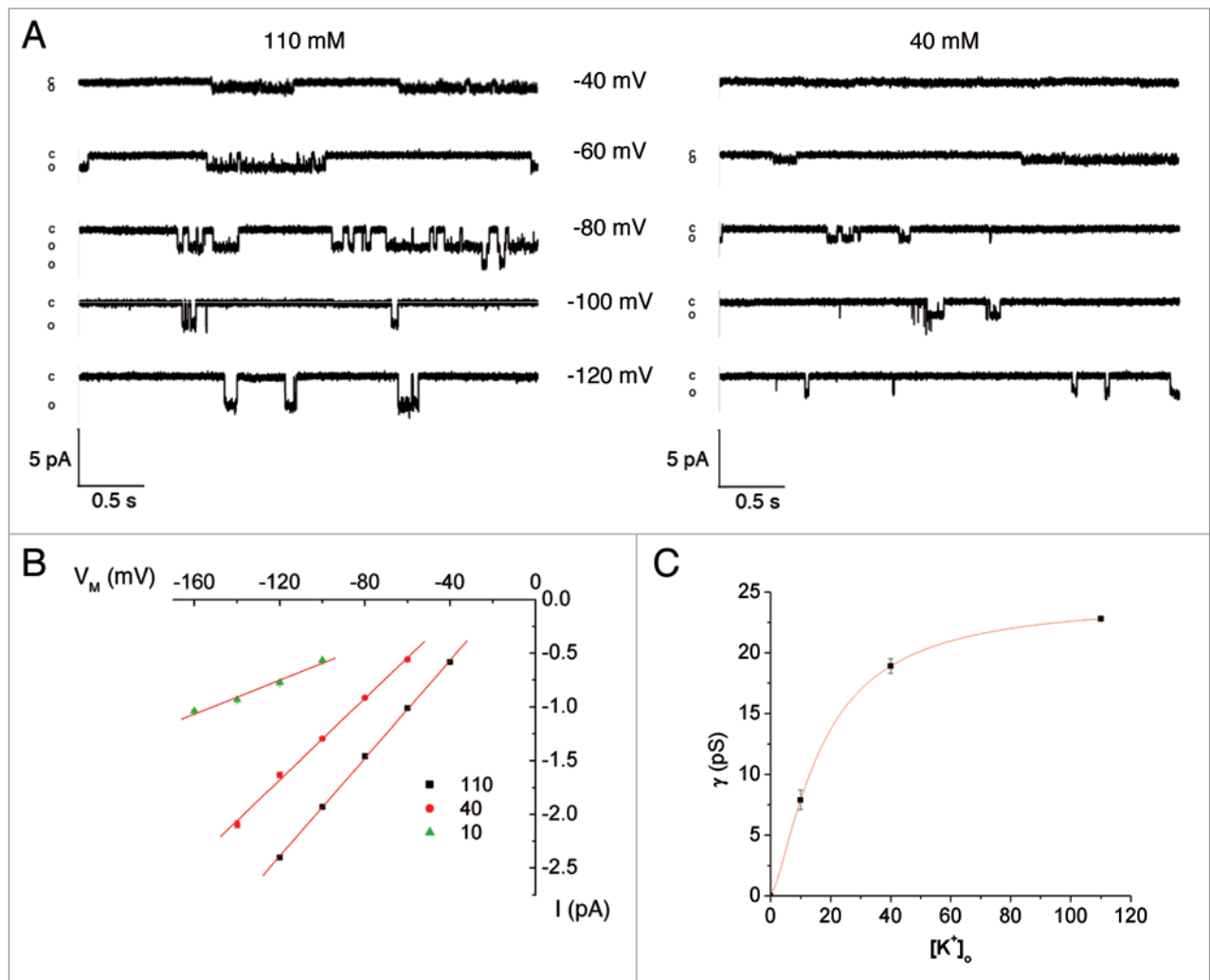
Figure 7. Effect of $[K^+]_o$ on Kir4.1 single channel conductance. (A) Representative current traces in cell-attached patches with 110 or 40 mM K^+ in the pipette as indicated. (B) i-V relationships at the indicated $[K^+]_{pipette}$. (C) Single-channel conductance as a function of $[K^+]_o$. The curve represents the best fit to the equation: $g = g_{max}/(1 + (K_{1/2}/[K])^n)$ where: $K_{1/2} = 16.7$ mM, $g_{max} = 24.4$ pS and $n = 1.4$.

also be inhibited by an ion present at the S0 site by repelling any ion entering S1. Effectively, this would mean that in our model (**Fig. 6A and B**) states (or groups of states) B, C and E would prevent deactivation of the channel. In fact, this combination of states shows the strongest dependency on the $[K^+]_o$ (**Sup. Fig. 1B**).

The Cs^+ data could be explained by increases in either S1/S3 or S2/S4 occupancy (**Sup. Table 1**). However, structural information using ion replacement in KcsA show minimal occupancy of S2 by Cs^+ indicating that the fit with favorable S1/S3 binding sites, and $[Cs^+]$ dependent increase in S1/S3 occupancy, might be more accurate.[45] In line with this, MD simulations have also shown that S2 is the most selective site.[13,46] Zhou and MacKinnon also showed that Rb^+ does not bind in the S2 site either.[45] Both Cs^+ and Rb^+ are, however, able to upregulate Kir4.1 (**Fig. 4**) and Kir1.1.[7] Rb^+ is also able to prevent inactivation of KcsA[47] and Shaker.[19]

Lack of structural information on NH_4^+ in the selectivity filter makes it unclear how this ion fits into this scheme. In our model substituting K^+ with NH_4^+ in the bath solution lead to a decrease

of S1/S3 occupancy, consistent with the idea that occupancy at these sites is important for channel activity. Substituting NH_4^+ did however also lead to an increase in S0 occupancy, which argues that S0 occupancy is insufficient to maintain the channel in an active state. It is possible that NH_4^+ interacts very differently with the selectivity filter than does K^+, invalidating our modeling process. However, our results make it clear that the peculiar properties of NH_4^+ can be explained if NH_4^+ experiences a different energetic landscape inside the pore rather than a fundamentally different permeation process.

In Kir1.1 it has been proposed that K^+-dependent regulation occurs due to closure of the selectivity-filter similar to C-type inactivation of KcsA.[10,18] C-type inactivation, or slow inactivation, was originally observed and studied in Shaker,[19,43,48] and later it was found that a similar process occurs in KcsA.[49] The rate of inactivation is on the order of seconds, and slows down in the presence of permeant extracellular cations.[19,47] Detailed structural studies of KcsA [11,14,45] and the computational studies that this information enabled,[16,21,22] provide good evidence that C-type
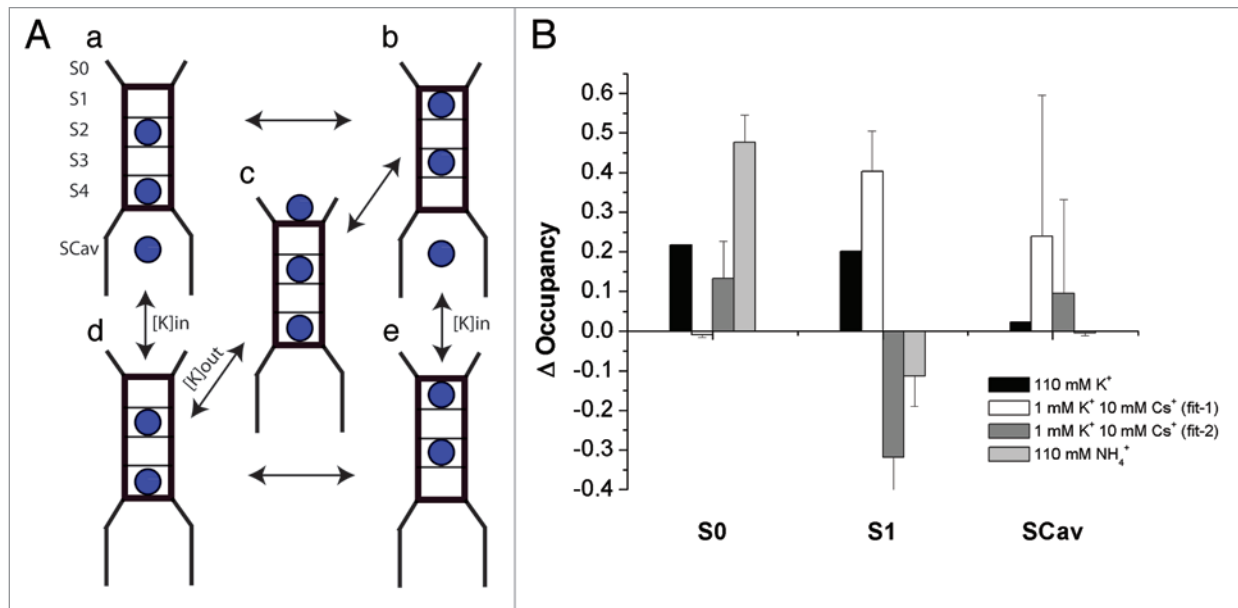
Figure 8. Kinetic model of K-channel permeation. (A) Cartoon of the one-ionic-species 6-site model. (B) Summary for the changes in occupancy, calculated as the fractional occupancy in the test solution-fractional occupancy in 1 mM K$^+$.

inactivation, at least in KcsA, involves a conformational change of the selectivity filter that closes the channel. The similarities in the dependence of external cations, combined with findings that mutations in the selectivity filter region affect K$^+$-dependent regulation of Kir1.1 has lead to the proposal that a similar mechanism occurs in inward rectifiers.[8-10]

For Kir1.1 it has been proposed that a secondary gate at the selectivity filter only closes once the pH$_i$-sensitive (bundle-crossing) gate has closed.[7,10,17,18,26] A similar relationship between the bundle-crossing gate and the selectivity-filter gate is believed to exist in K$_v$ channels[50] as well as KscA.[51,52] However, in these cases, opening the bundle-crossing gate leads to closure of the selectivity-filter gate. In Kir4.1, these gates appear to operate independently of each other. This conclusion is based both on the lack of effect of K^+_o on the response to cell pH (**Fig. 3A**) and on the persistence of the effect of K^+_o in a mutant channel that does not close with low internal pH (**Fig. 3B**). A similar lack of interaction between internal pH and external K$^+$ was found for Kir4.2 (Edvinsson, submitted).

In conclusion, we have found K^+_o-regulation in Kir-family member that is important in both neural and renal function. The recently described SESAME syndrome involves seizures and electrolyte imbalances due to loss-of-function mutations in Kir4.1.[53-57] We suggest that activation by K^+_o may play a role in the regulation by glial cells of extracellular K$^+$ in the brain.

Methods

Channel expression. Human Kir4.1 cDNA cloned into the pGEMHE-vector (a kind gift from Dr. Diomedes Logothetis) was linearized with NheI restriction enzyme (New England Biolabs, Ipswish, MA) and cRNA was made using mMESSAGE mMACHINE T7 kit (Ambion, Austin, TX).

Oocyte preparation. Oocytes were harvested from *Xenopus laevis* with approval of and in accordance with the guidelines of the IACUC of Weill Cornell Medical College. The animals were anesthetized through immersion into 1 L of tap water containing 1.5 gL^{-1} tricaine methanesulphonate and HEPES (adjusted to pH 7.4). A small incision was made in the abdomen and part of the ovary removed. Oocytes were dissociated by incubation in OR2 solution (in mM: NaCl 82.5, KCl 2.5, CaCl$_2$ 1, MgCl$_2$ 1, Na$_2$HPO$_4$ 1, HEPES 5 pH 7.4) containing 2 mgml^{-1} collagenase type II (Worthington) and 2 mgml^{-1} hyaluronidase type II (Sigma-Aldrich) and incubated with gentle shaking for 60 min. Oocytes were then injected with 10 ng of RNA and incubated in L-15 solution supplemented with HEPES (pH adjusted to 7.45), penicillin 63 mgL^{-1} and streptomycin 145 mgL^{-1} in 16°C overnight. All chemicals were from Sigma-Aldrich unless otherwise noted.

Mutagenesis. Site-directed mutagenesis was performed using the HotStar High Fidelity Polymerase kit (Qiagen, Hilden, Germany) according to the manufacturer's instructions. Primers were synthesized by Operon Technologies, Inc., (Huntsville, AL). The cDNA were sequenced by the Cornell University Bio Resource Center (Ithaca, NY, USA).

Two-electrode voltage clamp. For all experiments involving changes in [K$^+$]$_o$ the oocytes were incubated in the initial recording solution for 1 h prior to being placed in TEVC recording chamber. All recording solutions contained (in mM): 2 CaCl$_2$, 1 MgCl$_2$, 5 HEPES. Solutions with variable [K$^+$]$_o$ (in mM) 1 K, 4 K, 10 K, 40 K, 110 K were osmotically balanced by NaCl so that KCl + NaCl = 110. Other solutions contained (in mM): NMDG: 1 KCl, 109 NMDG; Rb: 110 Rb; Cs: 1 KCl 109 Na 10 CsCl; Ba: 1 KCl, 109 NaCl, 5 BaCl$_2$; Na: 1 KCl, 109 NaCl; NH$_4$: 110 NH$_4$Cl. The pH was adjusted to 7.4 for these solutions.

For the pH-sensitivity experiments the solutions contained (in mM): 2 CaCl$_2$ 1 MgCl$_2$ 5 HEPES and either 55 KCl and

55 KAcetate, or 10 KCl, 45 NaCl and 55 NaAcetate. The pH_i was calculated from the pH_o as previously described,[25] using the formula $pH_i = 0.595 \times pH_o + 2.4$. Whole-cell currents were measured in intact oocytes using a two-electrode voltage clamp (OC-725, Warner Instrument Corp.,) with ITC-16 interface (Instrutech) running Pulse software (Heka Elektronik). Pipettes were made from haematocrit capillary tubes (Fisher Scientific) with a three-step vertical pipette puller. Pipette resistances were 0.5–1 MΩ, when filled with 3 M KCl. Steady-state current-voltage curves were generated from a step-voltage protocol consisting of 26 pulses lasting 50 ms from -150 to +100 mV, from a holding potential set to the resting membrane potential.

Patch clamp. For single-channel measurements the vitelline membrane was mechanically removed from the oocytes in a hypertonic 110 mM K$^+$ bath solution containing 200 mM sucrose. The bath solution contained (in mM) 110 KCl, 2 CaCl$_2$, 1 MgCl$_2$, 5 HEPES, pH 7.4. The pipet solution contained (in mM) either 110 mM KCl, 40 mM KCl and 70 mM NaCl, or 10 mM KCl and 100 NaCl. All pipette solutions contained (in mM): 1 MgCl$_2$ and 5 HEPES, at pH 7.4. Patch-clamp pipets were prepared from hematocrit capillary glass (Fisher Scientific) using a vertical puller and fire polished with a microforge to yield resistances of 1–5 MΩ. Currents were recorded using an EPC-7 patch-clamp amplifier (Heka Elektronik) and digitized with a Digidata 1332A interface (Axon Instruments). Data were filtered at 0.5 kHz and analyzed with pCLAMP9 software (Axon Instruments). For analysis, data were filtered at 1 kHz, and analyzed using Pulsefit software (HEKA Elektronik).

Kinetic modeling. The model shown in **Figure 8** was evaluated using Matlab 7.8.0. The rate constants were calculated based on the values set for binding energies, energy barriers and electrical distances. For example, for k_{DE}, the transition between D and E:

$$k_{DE} = Q \cdot \exp^{(-(\Delta G_{12} - E_2 + \Delta G_{34} - E_4)}$$

Eqn. 1

where ΔG_{XY} is the height of the energy barrier between sites X and Y, E_X is the binding energy for site S_X, and Q is the frequency factor arbitrarily set to 1 x 10^9. The reverse rate constant was then calculated:

$$k_{ED} = k_{DE} \cdot \exp^{((E_1 + E_3) - (E_2 + E_4))}$$

Eqn. 2

A repulsion energy between the ion in the cavity and S4, E_r (2 R·T), was added to state A. A voltage dependence was added to each of the rate constants. For example:

$$k'_{DE} = k_{DE} \cdot \exp^{(\delta_3 \cdot Vm \cdot \frac{F}{R \cdot T})}$$

$$k'_{ED} = k_{ED} \cdot \exp^{-(\delta_3 \cdot Vm \cdot \frac{F}{R \cdot T})}$$

Eqn. 3

where δ_3 indicates the fraction of the electric field that needs to be crossed to reach the site from the neighboring site (**Fig. 9C**). The values for δ_1, δ_2 and δ_3 were 0.07, 0.113, 0.233, respectively, as used in a previous study of KcsA channels.[40] V_m is the membrane potential in volts, F is Faraday's constant, R is the ideal gas constant, and T is temperature in degrees Kelvin. In the above example, the transition involves movement of two ions the electrical distance, δ_3. The voltage dependence was partitioned equally between the forward and reverse rate constants. The rates were then entered into a rate matrix and solved for the steady-state occupancy.

The model with two ionic species was solved using the same approach with a separate set of parameters for binding energy and energy barriers used for Cs$^+$ or NH$_4$$^+$. The model was fitted to the appropriate experimental data using MatLab's built in *lsqcurvefit* function. To minimize the effect of the initial values provided to the fitting routine, each fit was repeated 10–100 times, with the initial values randomized each time. The numbers for the fit in **Supplemental Table 1** are given as mean ± SD. The K$^+$ single-channel data points used to fit the model were corrected for offsets from the predicted reversal potential.

Note

Supplemental materials can be found at:
www.landesbioscience.com/journals/channels/article/15827

References

1. Hibino H, Inanobe A, Furutani K, Murakami S, Findlay I, Kurachi Y. Inwardly rectifying potassium channels: their structure, function and physiological roles. Physiol Rev 2010; 90:291-366.

2. Zhang YY, Sackin H, Palmer LG. Localization of the pH gate in Kir1.1 channels. Biophys J 2006; 91:2901-9.

3. Schulte U, Fakler B. Gating of inward-rectifier K$^+$ channels by intracellular pH. Eur J Biochem 2000; 267:5837-41.

4. Schulte U, Hahn H, Wiesinger H, Ruppersberg JP, Fakler B. pH-dependent gating of ROMK (Kir1.1) channels involves conformational changes in both N and C termini. J Biol Chem 1998; 273:34575-9.

5. Sackin H, Nanazashvili M, Palmer LG, Krambis M, Walters DE. Structural locus of the pH gate in the Kir1.1 inward rectifier channel. Biophys J 2005; 88:2597-606.

6. Pearson WL, Dourado M, Schreiber M, Salkoff L, Nichols CG. Expression of a functional Kir4 family inward rectifier K$^+$ channel from a gene cloned from mouse liver. J Physiol 1999; 514:639-53.

7. Doi T, Fakler B, Schultz JH, Schulte U, Brandle U, Weidemann S, et al. Extracellular K$^+$ and intracellular pH allosterically regulate renal Kir1.1 channels. J Biol Chem 1996; 271:17261-6.

8. Sackin H, Syn S, Palmer LG, Choe H, Walters DE. Regulation of ROMK by extracellular cations. Biophys J 2001; 80:683-97.

9. Sackin H, Nanazashvili M, Li H, Palmer LG, Walters DE. An intersubunit salt bridge near the selectivity filter stabilizes the active state of Kir1.1. Biophys J 2009; 97:1058-66.

10. Schulte U, Weidemann S, Ludwig J, Ruppersberg J, Fakler B. K$^+$-dependent gating of Kir1.1 channels is linked to pH gating through a conformational change in the pore. J Physiol 2001; 534:49-58.

11. Doyle DA, Morais Cabral J, Pfuetzner RA, Kuo A, Gulbis JM, Cohen SL, et al. The structure of the potassium channel: molecular basis of K$^+$ conduction and selectivity. Science 1998; 280:69-77.

12. Berneche S, Roux B. A microscopic view of ion conduction through the K$^+$ channel. Proc Natl Acad Sci USA 2003; 100:8644-8.

13. Berneche S, Roux B. Energetics of ion conduction through the K$^+$ channel. Nature 2001; 414:73-7.

14. Zhou Y, Morais-Cabral JH, Kaufman A, MacKinnon R. Chemistry of ion coordination and hydration revealed by a K$^+$ channel-Fab complex at 2.0 A resolution. Nature 2001; 414:43-8.

15. Domene C, Klein ML, Branduardi D, Gervasio FL, Parrinello M. Conformational changes and gating at the selectivity filter of potassium channels. J Am Chem Soc 2008; 130:9474-80.

16. Berneche S, Roux B. A gate in the selectivity filter of potassium channels. Structure 2005; 13:591-600.

17. Sackin H, Vasilyev A, Palmer LG, Krambis M. Permeant cations and blockers modulate pH gating of ROMK channels. Biophys J 2003; 84:910-21.

18. Dahlmann A, Li M, Gao Z, McGarrigle D, Sackin H, Palmer LG. Regulation of Kir channels by intracellular pH and extracellular K$^+$: mechanisms of coupling. J Gen Physiol 2004; 123:441-54.

19. Lopez-Barneo J, Hoshi T, Heinemann SH, Aldrich RW. Effects of external cations and mutations in the pore region on C-type inactivation of Shaker potassium channels. Receptors Channels 1993; 1:61-71.

20. Cordero-Morales JF, Cuello LG, Perozo E. Voltage-dependent gating at the KcsA selectivity filter. Nat Struct Mol Biol 2006; 13:319-22.

21. Cordero-Morales JF, Cuello LG, Zhao Y, Jogini V, Cortes DM, Roux B, et al. Molecular determinants of gating at the potassium-channel selectivity filter. Nat Struct Mol Biol 2006; 13:311-8.

22. Cordero-Morales JF, Jogini V, Lewis A, Vasquez V, Cortes DM, Roux B, et al. Molecular driving forces determining potassium channel slow inactivation. Nat Struct Mol Biol 2007; 14:1062-9.

23. Fakler B, Schultz JH, Yang J, Schulte U, Brandle U, Zenner HP, et al. Identification of a titratable lysine residue that determines sensitivity of kidney potassium channels (ROMK) to intracellular pH. EMBO J 1996; 15:4093-9.

24. Schulte U, Hahn H, Konrad M, Jeck N, Derst C, Wild K, et al. pH gating of ROMK (K(ir)1.1) channels: control by an Arg-Lys-Arg triad disrupted in antenatal Bartter syndrome. Proc Natl Acad Sci USA 1999; 96:15298-303.

25. Choe H, Zhou H, Palmer LG, Sackin H. A conserved cytoplasmic region of ROMK modulates pH sensitivity, conductance and gating. Am J Physiol 1997; 273:516-29.

26. Rapedius M, Haider S, Browne KF, Shang L, Sansom MS, Baukrowitz T, et al. Structural and functional analysis of the putative pH sensor in the Kir1.1 (ROMK) potassium channel. EMBO Rep 2006; 7:611-6.

27. Somjen GG. Ion regulation in the brain: implications for pathophysiology. Neuroscientist 2002; 8:254-67.

28. Heinemann U, Lux HD. Ceiling of stimulus induced rises in extracellular potassium concentration in the cerebral cortex of cat. Brain Res 1977; 120:231-49.

29. Kofuji P, Newman EA. Potassium buffering in the central nervous system. Neuroscience 2004; 129:1045-56.

30. Walz W. Role of astrocytes in the clearance of excess extracellular potassium. Neurochem Int 2000; 36:291-300.

31. Takumi T, Ishii T, Horio Y, Morishige K, Takahashi N, Yamada M, et al. A novel ATP-dependent inward rectifier potassium channel expressed predominantly in glial cells. J Biol Chem 1995; 270:16339-46.

32. Olsen ML, Higashimori H, Campbell SL, Hablitz JJ, Sontheimer H. Functional expression of Kir4.1 channels in spinal cord astrocytes. Glia 2006; 53:516-28.

33. Kucheryavykh YV, Kucheryavykh LY, Nichols CG, Maldonado HM, Baksi K, Reichenbach A, et al. Downregulation of Kir4.1 inward rectifying potassium channel subunits by RNAi impairs potassium transfer and glutamate uptake by cultured cortical astrocytes. Glia 2007; 55:274-81.

34. Neusch C, Papadopoulos N, Muller M, Maletzki I, Winter SM, Hirrlinger J, et al. Lack of the Kir4.1 channel subunit abolishes K+ buffering properties of astrocytes in the ventral respiratory group: impact on extracellular K+ regulation. J Neurophysiol 2006; 95:1843-52.

35. Higashi K, Fujita A, Inanobe A, Tanemoto M, Doi K, Kubo T, et al. An inwardly rectifying K+ channel, Kir4.1, expressed in astrocytes surrounds synapses and blood vessels in brain. Am J Physiol Cell Physiol 2001; 281:922-31.

36. Poopalasundaram S, Knott C, Shamotienko OG, Foran PG, Dolly JO, Ghiani CA, et al. Glial heterogeneity in expression of the inwardly rectifying K(+) channel, Kir4.1, in adult rat CNS. Glia 2000; 30:362-72.

37. Rapedius M, Fowler PW, Shang L, Sansom MS, Tucker SJ, Baukrowitz T. H bonding at the helix-bundle crossing controls gating in Kir potassium channels. Neuron 2007; 55:602-14.

38. Xu H, Yang Z, Cui N, Chanchevalap S, Valesky WW, Jiang C. A single residue contributes to the difference between Kir4.1 and Kir1.1 channels in pH sensitivity, rectification and single channel conductance. J Physiol 2000; 528:267-77.

39. Yang Z, Jiang C. Opposite effects of pH on open-state probability and single channel conductance of kir4.1 channels. J Physiol 1999; 520:921-7.

40. Kutluay E, Roux B, Heginbotham L. Rapid intracellular TEA block of the KcsA potassium channel. Biophys J 2005; 88:1018-29.

41. Grabe M, Bichet D, Qian X, Jan YN, Jan LY. K+ channel selectivity depends on kinetic as well as thermodynamic factors. Proc Natl Acad Sci USA 2006; 103:14361-6.

42. Jiang Y, Lee A, Chen J, Cadene M, Chait BT, MacKinnon R. The open pore conformation of potassium channels. Nature 2002; 417:523-6.

43. Baukrowitz T, Yellen G. Modulation of K+ current by frequency and external [K+]: a tale of two inactivation mechanisms. Neuron 1995; 15:951-60.

44. Choi KL, Aldrich RW, Yellen G. Tetraethylammonium blockade distinguishes two inactivation mechanisms in voltage-activated K+ channels. Proc Natl Acad Sci USA 1991; 88:5092-5.

45. Zhou Y, MacKinnon R. The occupancy of ions in the K+ selectivity filter: charge balance and coupling of ion binding to a protein conformational change underlie high conduction rates. J Mol Biol 2003; 333:965-75.

46. Luzhkov VB, Aqvist J. K+/Na+ selectivity of the KcsA potassium channel from microscopic free energy perturbation calculations. Biochim Biophys Acta 2001; 1548:194-202.

47. Chakrapani S, Cordero-Morales JF, Perozo E. A quantitative description of KcsA gating I: macroscopic currents. J Gen Physiol 2007; 130:465-78.

48. Hoshi T, Zagotta WN, Aldrich RW. Two types of inactivation in Shaker K+ channels: effects of alterations in the carboxy-terminal region. Neuron 1991; 7:547-56.

49. Gao L, Mi X, Paajanen V, Wang K, Fan Z. Activation-coupled inactivation in the bacterial potassium channel KcsA. Proc Natl Acad Sci USA 2005; 102:17630-5.

50. Panyi G, Deutsch C. Cross talk between activation and slow inactivation gates of Shaker potassium channels. J Gen Physiol 2006; 128:547-59.

51. Cuello LG, Jogini V, Cortes DM, Pan AC, Gagnon DG, Dalmas O, et al. Structural basis for the coupling between activation and inactivation gates in K+ channels. Nature 2010; 466:272-5.

52. Cuello LG, Jogini V, Cortes DM, Perozo E. Structural mechanism of C-type inactivation in K+ channels. Nature 2010; 466:203-8.

53. Bockenhauer D, Feather S, Stanescu HC, Bandulik S, Zdebik AA, Reichold M, et al. Epilepsy, ataxia, sensorineural deafness, tubulopathy and KCNJ10 mutations. N Engl J Med 2009; 360:1960-70.

54. Scholl UI, Choi M, Liu T, Ramaekers VT, Hausler MG, Grimmer J, et al. Seizures, sensorineural deafness, ataxia, mental retardation and electrolyte imbalance (SeSAME syndrome) caused by mutations in KCNJ10. Proc Natl Acad Sci USA 2009; 106:5842-7.

55. Shi M, Zhao G. The EAST syndrome and KCNJ10 mutations. N Engl J Med 2009; 361:630.

56. Reichold M, Zdebik AA, Lieberer E, Rapedius M, Schmidt K, Bandulik S, et al. KCNJ10 gene mutations causing EAST syndrome (epilepsy, ataxia, sensorineural deafness and tubulopathy) disrupt channel function. Proc Natl Acad Sci USA 2010; 107:14490-5.

57. Sala-Rabanal M, Kucheryavykh LY, Skatchkov SN, Eaton MJ, Nichols CG. Molecular mechanisms of EAST/SeSAME syndrome mutations in Kir4.1 (KCNJ10). J Biol Chem 2010; 285:36040-8.